STEM CELLS TRANSLATIONAL MEDICINE®

CELL-BASED DRUG DEVELOPMENT, SCREENING, AND TOXICOLOGY

Comparison of Drug and Cell-Based Delivery: Engineered Adult Mesenchymal Stem Cells Expressing Soluble Tumor Necrosis Factor Receptor II Prevent Arthritis in Mouse and Rat Animal Models

LINDA N. LIU,[a] GANG WANG,[a] KYLE HENDRICKS,[a] KEUNMYOUNG LEE,[a] ERNST BOHNLEIN,[b] UWE JUNKER,[b] JOSEPH D. MOSCA[a]

Key Words. Adult stem cells • Arthritis • Chondrogenesis • Gene therapy • Immunodeficient mouse • Mesenchymal stem cells • SCID mice • sTNFR

[a]Osiris Therapeutics, Inc., Baltimore, Maryland, USA; [b]Novartis Institute for Biomedical Research, Basel, Switzerland

Correspondence: Joseph D. Mosca, Ph.D., JDM Technologies Inc., 4201 Blue Barrow Ride, Ellicott City, Maryland 21042, USA. Telephone: 443-831-9278; E-Mail: jdmosca@gmail.com

Received October 17, 2012; accepted for publication January 29, 2013; first published online in SCTM *EXPRESS* April 16, 2013.

1066-5099/2013/$20.00/0

http://dx.doi.org/10.5966/sctm.2012-0135

ABSTRACT

Rheumatoid arthritis (RA) is a systemic autoimmune disease with unknown etiology where tumor necrosis factor-α (TNFα) plays a critical role. Etanercept, a recombinant fusion protein of human soluble tumor necrosis factor receptor II (hsTNFR) linked to the Fc portion of human IgG1, is used to treat RA based on the rationale that sTNFR binds TNFα and blocks TNFα-mediated inflammation. We compared hsTNFR protein delivery from genetically engineered human mesenchymal stem cells (hMSCs) with etanercept. Blocking TNFα-dependent intercellular adhesion molecule-1 expression on transduced hMSCs and inhibition of nitric oxide production from TNFα-treated bovine chondrocytes by conditioned culture media from transduced hMSCs demonstrated the functionality of the hsTNFR construction. Implanted hsTNFR-transduced mesenchymal stem cells (MSCs) reduced mouse serum circulating TNFα generated from either implanted TNFα-expressing cells or lipopolysaccharide induction more effectively than etanercept (TNFα, 100%; interleukin [IL]-1α, 90%; and IL-6, 60% within 6 hours), suggesting faster clearance of the soluble tumor necrosis factor receptor (sTNFR)-TNFα complex from the animals. In vivo efficacy of sTNFR-transduced MSCs was illustrated in two (immune-deficient and immune-competent) arthritic rodent models. In the antibody-induced arthritis BalbC/SCID mouse model, intramuscular injection of hsTNFR-transduced hMSCs reduced joint inflammation by 90% compared with untransduced hMSCs; in the collagen-induced arthritis Fischer rat model, both sTNFR-transduced rat MSCs and etanercept inhibited joint inflammation by 30%. In vitro chondrogenesis assays showed the ability of TNFα and IL1α, but not interferon γ, to inhibit hMSC differentiation to chondrocytes, illustrating an additional negative role for inflammatory cytokines in joint repair. The data support the utility of hMSCs as therapeutic gene delivery vehicles and their potential to be used in alleviating inflammation within the arthritic joint. STEM CELLS TRANSLATIONAL MEDICINE *2013;2:000–000*

INTRODUCTION

Tumor necrosis factor-α (TNFα) is a central mediator in a wide spectrum of physiological functions with differential effects on immune and nonimmune cells in mediating normal homeostatic mammalian processes [1, 2]. TNFα is produced primarily as a type II transmembrane protein and is cleaved by the metalloprotease TNFα-converting enzyme to the soluble form [3, 4]. TNFα can activate and induce many cytokines, including interleukin (IL)-1, IL-6, IL-8, and granulocyte-macrophage colony-stimulating factor, and upregulate adhesion molecules on endothelial cells leading to leukocyte extravasation [5, 6]. Some of these molecules are presently being tested as potential surrogate markers for disease activities [7]. Within joint cavities, the TNFα-induced cytokine cascade originating from activated macrophages, T lymphocytes, and neutrophils, causes inflammation and joint destruction. The concept that TNFα is a major mediator of the inflammatory response in the affected joints of rheumatoid arthritis (RA) patients came from in vivo animal models where recombinant soluble TNFα receptors improve clinical symptoms and prevent joint destruction [8, 9], in addition to the observation that expression of an mRNA-stabilized TNFα gene leads to an RA condition that is prevented by administration of anti-TNF antibody [10]. More recently, a DNase II-null mouse model showed similar dependence on cytokine expression to induce arthritis and was reversed by anticytokine therapies [11]. The suggestive data from animal models on the central role of TNFα in RA have been substantiated in clinical trials [12, 13].

Signal transduction occurs when TNFα in a *trimeric* structure binds to one of its two receptors: p55 (TNF receptor I) or p75 (TNF receptor II) on the cell surface [14]. Although TNFα production is restricted to a small subset of cells, the two receptors are almost ubiquitously expressed. TNFα inhibitors containing the truncated form of the extracellular region of these receptors are naturally occurring in RA disease tissue and fluids where their presence correlates with disease activities [15]. One of these monomeric soluble receptors, p75 TNF receptor (TNFR), is a dimeric molecule linked to the immunoglobin Fc fragment (soluble tumor necrosis factor receptor [sTNFR]:Fc): etanercept (Enbrel; Immunex Corp., Thousand Oaks, CA, http://www.enbrel.com/HCP). This Ig-fusion molecule along with two monoclonal antibodies: infliximab (Remicade [Janssen Biotech, Inc., Horsham, PA, http://www.remicade.com], a murine monoclonal antibody linked to the constant domains of human kappa and immunoglobulin) and adalimumab (Humira [Abbott Laboratories, North Chicago, IL, http://www.humira.com], a human recombinant IgG1 monoclonal antibody) are currently the three TNFα inhibitors approved in the United States [16]. Other licensed TNFα blockers currently in use are certolizumab pegol (a PEGylated humanized monoclonal anti-TNFα Fab fragment) and golimumab (a humanized monoclonal anti-TNFα antibody). The pharmacologies of these agents differ in their binding properties of the soluble monomeric/trimeric and membrane-bound forms of TNFα with respect to ligand affinity, release, complex stability, and binding ratios [17, 18].

Although the current TNFα inhibitors are close mimics to the natural molecule, they are not targeted to their site of action within the body. In RA, these biologics are systemically delivered, requiring higher amounts of these inhibitors to treat affected arthritic joints and tissues in addition to affecting processes that are unintended cellular targets within the hematopoietic lineage. These unintended complications affect successful progenitor engraftment [19], augmentation of human T lymphopoiesis [20], immunity toward bacterial pathogens [21, 22], and antitumor immunity [23]. These side effects result in defective humoral immune responses [24] and regulatory T-cell function [23] that are reminiscent of toxicities found with traditional small molecule drugs. Moreover, biologics in general require intense development and manufacturing processes that are challenging for reproducibility, even within the same company (see [25] and [26] on the reformulation of EPREX in Europe).

Vehicles have been devised to target the biologics to specific areas. These include synthetic polymers, in addition to viruses and cells. However, synthetic polymer/nanotechnology [27] approaches often require biological molecules, raising concerns on immunogenicity and comparability. Viruses for gene therapy/gene delivery require infection and integration that can lead to insertional mutagenesis (murine leukemia virus [MuLV], lentivirus), immunogenicity (adeno-associated virus [AAV]), cytotoxicity (herpes simplex virus), and promoter inactivation. Cells, especially mesenchymal stem cells (MSCs), with their ability to differentiate into cartilage/bone, may have the best potential for arthritis treatment. These cells can be genetically modified without loss of differentiation capability [28] and with intrinsic immune suppressive behavior, which allows allogeneic transplantation [29, 30].

In this report, we furthered the development and characterization of an alternative approach to recombinant protein therapy using human mesenchymal stem cell (hMSC)-based delivery. We demonstrated by comparison with recombinant protein injections (benchmarked to etanercept) that a single intramuscular injection of sTNFR-transduced hMSCs can result in a faster clearance of lipopolysaccharide (LPS)-induced TNFα and associated cytokine cascade in mice, resulting in 100% removal of TNFα, 90% of IL-1α, and 60% of IL-6 within 6 hours of the LPS insult. Efficacy models in mice showed that sTNFR-expressing hMSCs protected the animals against antibody-induced arthritis compared with nonmodified hMSCs and in rats showed comparable reduction to etanercept in paw inflammation caused by collagen-induced arthritis.

Methods and Materials

Isolation and Cultivation of Primary hMSCs

The procedures for isolation and cultivation of primary hMSCs were described previously [31–33]. The hMSCs (154, 219, and 225) used in these studies were collected from three healthy human donors (age 28–46 years) at the Johns Hopkins Oncology Center under an institutional review board-approved protocol.

Generation of Human sTNFR Retroviral Vectors, Packaging Cell Lines, and Transduction of hMSCs

The human soluble tumor necrosis factor receptor type II (hsTNFR) was obtained using specific oligonucleotide primers (O-OT2065 [5′-ctcgagCCCCGCCCGCACCCatgGCGCCCGTCGCCGTC] containing an XhoI site and O-OT3111 [5′-GATCggatccGTCGC-CAGTGCTCCCTTCAGCTGGGGGGCTGGG] containing a BamHI site) and reverse transcription-polymerase chain reaction (PCR) amplification from poly(A^+) human kidney RNA (Clontech, Mountain View, CA, http://www.clontech.com). The amplified product was cloned into pCR2.1-TOPO (Invitrogen, Carlsbad, CA, http://www.invitrogen.com) and sequenced to confirm identity, resulting in the plasmid pOT109B. The human IgG Fc domain was PCR-amplified from plasmid pcDNA3 (Invitrogen) using O-OT490 (5′-GAGAgtcgacTCATTTACCCGGAGACAG) containing a SalI site and O-OT489 (5′-GAGAggatccGGTGGTGGTGGTTCTTCTTCTTGT-GACAAAACTCACAC) containing a BamHI site and then subcloned into pJM573Neo [31] to form pOT52. The constructed hsTNFR sequence was removed from pOT109B by digestion with XhoI and BamHI and then subcloned into the pOT52 XhoI and BamHI sites to form pOT110. The plasmid (pOT110) containing the coding region for the hsTNFR together with human IgG Fc domain (a 1.5-kilobase [kb] fragment) was digested with restriction enzymes XhoI and SalI, and the purified hsTNFR-Ig fragment was inserted into the retroviral vector pLiG at the unique XhoI site (pLiG; provided by Dr. Gabor Veres; Novartis International, Basel, Switzerland, http://www.novartis.com). The pLiG vector contains the enhanced green fluorescent protein (eGFP) behind an internal ribosome entry sequence (IRES). The resulting retroviral vector construction, pOT298 (Fig. 1A), was cotransfected together with pCIGP (provided by Dr. Richard Rigg, Norvartis, a plasmid encoding the Moloney murine leukemia virus *gag*/*pol* gene); and pCIGL (a plasmid encoding the vesicular stomatitis virus G glycoprotein envelope) using the FuGENE 6 transfection reagent into 293 cells, and the supernatant virus made from this transient transfection was used to transduce the ProPak-A packaging cell line [34]. Flow cytometric analysis of the transduced ProPak-A cell line revealed a 5% green fluorescent protein (GFP)-positive population. This population was enriched by two rounds

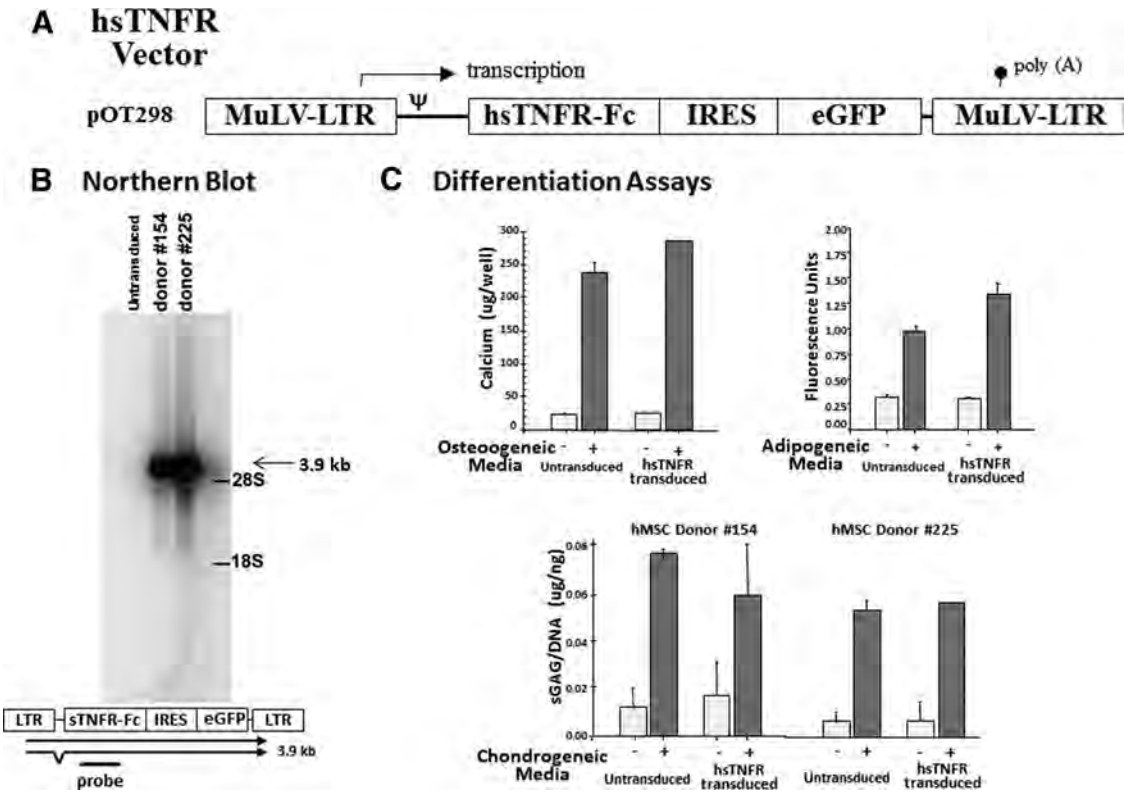

Figure 1. Vector construction/expression and cellular differentiation potential for transduced human mesenchymal stem cells (hMSCs). **(A):** Schematic representation of the retroviral vector LTNFRiG. Transcription of the hsTNFR-Fc gene is initiated from the 5′ LTR indicated by an arrow. The packaging signal (Ψ) is indicated. Translation of the eGFP is directed by IRES. The vector is not drawn to scale. **(B):** Northern blot analysis of transgene hsTNFR integration. Equal amounts of total RNA from mock or hsTNFR-transduced hMSCs (two donors, 154 and 225) were analyzed with a radiolabeled hsTNFR-specific probe. The migration of 28 and 18 S rRNA is shown on the right. **(C):** hsTNFR-transduced hMSCs retain the capacity for osteogenic, adipogenic, and chondrogenic differentiation. For osteogenic differentiation, untransduced and hsTNFR-transduced hMSCs (donor 225, p4) were cultured in control (−) or osteogenic (+) medium. Calcium deposition in triplicate wells was assayed after 18 days. The average and the standard error of the mean are presented for each culture condition. Similar results were obtained for hMSC donor 154. For adipogenic differentiation, untransduced and hsTNFR-transduced hMSCs were cultured in control or adipogenic medium. Nile Red retention fluorescence in each well was assayed in triplicate. For chondrogenic differentiation, untransduced and hsTNFR-transduced hMSCs were cultured in control (−) or chondrogenic (+) medium. GAG production was assayed in triplicate after 21 days in pellet culture. The average and the standard deviation are presented for each culture condition. The data shown are for donor 225, P4; similar results were obtained for hMSC donor 154. Abbreviations: eGFP, enhanced green fluorescent protein; GAG, sulfated glycosaminoglycans; hsTNFR, human soluble tumor necrosis factor receptor II; IRES, internal ribosome entry sequence; LTR, long terminal repeat; MuLV, murine leukemia virus.

of cell sorting to produce a greater than 90% eGFP-positive cell population. The ProPak-pOT298 producer cell line was cultured, and retroviral supernatants were collected for hMSC transduction; transduction efficiency was assessed on NIH3T3 cells for eGFP flow cytometry and sTNFR expression. Transduction of hMSCs was performed according to the standard protocol of centrifugation as described previously [28, 31]. Transduced hMSCs were analyzed by Northern blot analysis (Fig. 1B) and tested for their ability to undergo osteogenic, adipogenic, and chondrogenic differentiation (Fig. 1C).

Functional In Vitro Characterization of hsTNFR-Transduced hMSCs

Northern Blot Analysis

Poly(A^+) RNA was isolated from untransduced and hsTNFR-transduced hMSCs using the Oligotex mRNA isolation kit (Qiagen, Hilden, Germany, http://www.qiagen.com) according to the manufacturer's protocol. Poly(A^+) RNA (3 μg) was analyzed by electrophoresis on 1% agarose/formaldehyde gels, transferred to nylon membranes, and hybridized with a hsTNFR-specific random priming labeled probe. The filters were washed for several hours at 65°C in 0.2× standard saline citrate/0.5% SDS and exposed to XAR-5 film (Kodak, Rochester, NY, http://www.kodak.com) at −80°C.

Adult Stem Cell Differentiation Assays

Cell proliferation was measured in cultures using a modification of the crystal violet dye-binding method. The osteogenic differentiation assay was performed as previously reported [35]. Calcium deposition was measured after 2 weeks of culture in osteogenic-supplemental medium. Calcium was extracted from cells by shaking for 4 hours at 4°C and then centrifugation at 1,000*g* for 5 minutes. The supernatant was used for calcium determination according to the manufacturer's instructions contained in Sigma Kit 587 (Sigma-Aldrich, St. Louis, MO, http://www.sigmaaldrich.com). The adipogenic differentiation assay was performed as previously reported [36]. The accumulation of intracellular triglyceride droplets was visualized by staining with Oil Red O and quantified by Nile Red fluorescence. The cells were grown in six-well plates, fixed in 10% neutral buffered formalin at

room temperature, and incubated for 15 minutes with 0.2% saponin, 8 μg/ml 4′,6-diamidino-2-phenylindole, and 1 μg/ml Nile Red in phosphate-buffered saline (PBS) at room temperature. Fluorescence was measured with a fMAX Fluorescent Microplate Reader (Molecular Devices Corp., Union City, CA, http://www.moleculardevices.com) using 355/460- and 485/538-nm filter sets. The chondrogenic differentiation assay was performed as previously reported [37]. The accumulation of sulfated glycosaminoglycans (s-GAGs) in chondrogenic pellets was measured by a dye-binding method using dimethylmethylene blue. To normalize the values of s-GAG, the amount of DNA in the chondrogenic pellets was determined with Picogreen fluorescent dye (Molecular Probes, Eugene, OR, http://probes.invitrogen.com) according to the manufacturer's instructions. Histological evaluation of the pellets were performed by staining proteoglycans in the pellet with Safranin-O and type II collagen with a monoclonal antibody (C4F6). Human MSCs were either left untreated or treated with 10 μg/ml TNFα, 10 μg/ml IL-1α, or 10 μg/ml interferon (IFN) γ for 24 hours before pelleting for the chondrogenic differentiation assay and histological evaluation.

Fluorescence-Activated Cell Sorting Analysis

Cell sorting (ProPak-A) was performed on a Coulter EPICS flow cytometer (Beckman Coulter, Fullerton, CA, http://www.beckmancoulter.com) equipped with a 488-nm argon laser. The gates were set based on forward and side scatter (cell size and granularity) and for viability based on the exclusion of propidium iodide. Positive events for the emission of eGFP were collected using a 525-nm band pass filter. Analysis of eGFP fluorescence of transduced hMSCs was performed by flow cytometry as previously reported [33]. Briefly, the transduced cells were washed twice with Dulbecco's phosphate-buffered saline (D-PBS) and detached from the culture vessels by incubation with 0.05% trypsin-EDTA (Life Technologies, Rockville, MD, http://www.lifetech.com). The cells were recovered by centrifugation and washed twice with D-PBS. Then the cells were resuspended in D-PBS with 1% paraformaldehyde (Electron Microscopy Sciences, Fort Washington, PA, http://www.emsdiasum.com) immediately before being analyzed. Nonspecific fluorescence was determined using untransduced hMSCs. The samples were analyzed by collecting 10,000 events on a Vantage instrument using Cell-Quest software (Becton, Dickinson and Company, Franklin Lakes, NJ, http://www.bd.com).

Cytokine and sTNFR Measurements

Conditioned medium was collected from cultures of either untransduced or hsTNFR-transduced hMSCs. For detection at each cell passage, 1×10^6 cells were seeded into T-185 flasks in 30 ml of medium. A 1-ml aliquot of conditioned medium was removed after 24 hours and assayed for hsTNFR by enzyme-linked immunosorbent assay (ELISA; R&D Systems Inc., Minneapolis, MN, http://www.rndsystems.com). For in vitro and in vivo hsTNFR secretion, ELISA analysis was performed on transduced cell culture medium or mouse plasma using hsTNFR, mouse TNFα, mouse IL-1α, and mouse IL-6 ELISA kits from R&D Systems. The standard supplier's protocols were followed, and absorbance at 450 nm with 570-nm reference was analyzed by software ThermoMax with a ThermoMax microplate reader (Molecular Devices). All of the samples were analyzed in duplicate. The sample average (pg/ml) was determined based on a standard curve generated for each assay.

Nitric Oxide Release From Human TNFα-Treated Bovine Chrondrocytes

This assay was performed using human TNFα and IL-1α as the nitric oxide (NO)-stimulating agent as previously described [38] in undiluted hsTNFR-transduced hMSC conditioned medium. Briefly, bovine articular chondrocytes (BACs) were cultured 5 days before untransduced or hsTNFR-transduced hMSCs culture supernatant was added to BAC together with 10 ng/ml of human TNFα or 10 ng/ml of IL-1α. Conditioned medium was collected 24 hours later and tested for NO production by a commercially available total NO kit from R&D Systems. Media from four different donor MSCs were tested.

Human TNFα-Dependent Surface Intercellular Adhesion Molecule-1 Expression

Two hundred thousand untransduced or hsTNFR-transduced hMSCs were seeded into six-well plates and cultured overnight. New media plus 0, 1, 5, 50, 100, and 200 units/ml of human TNFα (R&D Systems) were added to each well, and the cultures were incubated for 3 days. The cells were harvested from the plates with 0.05% trypsin and washed twice with D-PBS. The cells were then resuspended in 200 μl of D-PBS containing anti-intercellular adhesion molecule (ICAM)-1 monoclonal antibody conjugated with phycoerythrin purchased from Pharmingen (San Diego, CA) and incubated in the dark for 30 minutes. After two washes with D-PBS, the ICAM-1 positive cells were quantified by fluorescence-activated cell sorting (FACS).

Functional In Vivo Characterization of hsTNFR-Transduced hMSCs

Matrix and Nonmatrix Implantation of hMSCs Into NOD/SCID mice

All animal experimentation was conducted under an institutional review board-approved protocol. NOD/SCID mice were obtained (Jackson Laboratory, Bar Harbor, ME, http://www.jax.org), and colonies were established in-house. The cells were delivered unattached by i.m. or s.c. routes, or attached to various matrices, for example, polyglycolide (PGA) felt pads, CultiSpher G beads, hydroxyapatite (HA)/β-tricalcium phosphate (TCP) (65:35%) ceramic cubes, and alginate disks and then implanted i.m. or s.c. Nonconditioned animals were anesthetized with Nembutal (1.5 mg per mouse, i.p.) in preparation for hMSC implantation. For i.m. or s.c. injections of cells alone, hMSCs were injected using a 1-ml syringe with a 27-gauge needle. The cells (2×10^6) were resuspended in 100 μl of serum-free Opti-MEM, and 50 μl of the cell suspension was injected into either the quadriceps on each thigh of the animal or just under the skin in the back. For PGA felt pad (Albany International Research Comp., Inc., Mansfield, MA, http://www.albint.com) implantation, the material was sliced to a size of 5 mm^2. The sliced PGA pieces were first soaked in 100% ethanol for 30 minutes; then rehydrated for 5–10 minutes through 100%, 75%, 50%, and 25% ethanol/PBS serials; and finally soaked for 30 minutes in serum-free Opti-MEM (Life Technologies) twice before being dried on sterile gauze pads. Human MSCs were resuspended in 100 μl of Opti-MEM and loaded onto PGA. Loaded pads were transferred to a Petri dish and incubated for 1 hour at 37°C with 10% CO_2. Prior to transplantation, the mice were shaved on their lower back, and the cell-loaded pads were implanted after a 1-cm incision was made along the dorsum according to aseptic surgical techniques. Blunt dissection was then used to separate the cutaneous tissues to form a

pocket under the skin into which the felt pads were implanted. After implantation, the skin incision was passively closed with stainless steel skin staples around the implants. CultiSpher G beads (DG-0001-00; HyClone, Logan, UT, http://www.hyclone.com), collagen-based macroporous microcarriers, were prepared according to the manufacturer's recommendations. Briefly, 0.1 g (dry weight) of microcarriers were rehydrated in 5 ml of Ca^{2+}- and Mg^{2+}-free PBS for 1 hour and sterilized by autoclaving. Sterilized microcarriers were washed with PBS and cell culture medium and then stored at 4°C in the cell culture medium. For cell seeding, the microcarriers were prewarmed to 37°C and incubated with medium-washed detached trypsinized cells for 1 hour; microcarrier attached cells were collected by allowing the carriers to settle for 15 minutes in a 15-ml conical tube. For 200–450-μm mean pore size HA/TCP ceramic cubes (provided by Zimmer, Warsaw, IN, www.zimmer.com), hMSCs were attached as described [39]. Briefly, HA/TCP ceramic cubes ($3 \times 3 \times 3$ mm) were sterilized by baking at 250°C overnight followed by incubations with fibronectin (200 μg/ml) for 16 hours at 4°C. The coated cubes were first dried at room temperature and then combined with harvested hMSCs in Dulbecco's modified Eagle's medium with low glucose (2.5×10^6 cells per milliliter) at 37°C for 4 hours with occasional shaking. The number of cells per ceramic cube is estimated at 0.5×10^6 cells per cube as determined by the number of cells remaining in suspension. Lastly, cell attached alginate disks (Keltone LCVR; Kelco Corp., San Diego, CA, http://www.cpkelco.com; two or three 10-mm-diameter disks) were surgically implanted s.c.

Sera Collection From NOD/SCID Mice

Because of the fragility and size of the NOD/SCID mouse, each week, 100–150 μl of blood was collected following an institutional animal care and use committee-approved animal protocol by retro-orbital puncture into heparinized capillary tubes (Becton Dickinson; catalog no. 420317) from Nembutal-anesthetized (2 mg per mouse) animals; plasma from five animals was pooled together for the hsTNFR and cytokine ELISAs.

Expression and Neutralization of Human TNFα in NOD/SCID Mice

Human MSCs were transduced with a retroviral vector expressing human TNFα and an IRES-neomycin selectable marker (pOT138). Human TNFα transduced hMSCs (5×10^6 cells) were injected i.p. into 10 animals and compared with 10 animals injected i.p. with untransduced hMSCs. Each group was split in half (five animals each) and injected s.c. (5×10^6 cells) with either hsTNFR-transduced hMSCs or untransduced hMSCs. This resulted in four groups with five animals each. TNFα and hsTNFR concentrations in the sera of the animals were determined as described above.

LPS Induction and Modulation of Mouse Cytokines

LPS (Sigma-Aldrich) was suspended in double-distilled H_2O to a concentration of 2.5 mg/ml and stored at 4°C. Two or three weeks before LPS challenge, NOD/SCID mice (Jackson Laboratory; 8 weeks old, approximately 25 g) were implanted with PGA loaded with control or hsTNFR-transduced hMSCs (4×10^6 cells per mouse). The mice were i.p. injected with a sublethal dosage of LPS (20 mg/kg). Five to ten mice from each group were sacrificed prior to LPS challenge or at 1 and 6 hours post-LPS challenge. Total blood was collected by cardiac puncture. Briefly, the mice were euthanized with CO_2, the heart was exposed, and a 1-ml syringe with a 25-gauge needle (rinsed with 10,000 units/ml heparin) was inserted directly into the heart. Blood was withdrawn into the syringe and transferred into a 1.5-ml microcentrifuge tube. The plasma was collected after centrifugation (4 minutes, 6,000 rpm) and aliquot and stored at −80°C for hsTNFR, mouse TNFα, mouse IL-1α, and mouse IL-6 ELISAs.

Arthritic Rodent Models

Antibody-Induced Arthritis

Young BalbC/SCID mice (Jackson Laboratory; 6–7 weeks old, approximately 20 g) were i.m. injected with control or hsTNFR-transduced hMSCs as described above. Four days later, the mice were i.v. infused with 300 μl (3 mg total) of anti-type II collagen monoclonal antibody cocktail (Chondrex, Redmond, WA, www.chondrex.com) by tail vein injection. Within 24–48 hours, the mice were administered 50 μg of LPS (in 200 μl) i.p. The mice were monitored daily. Arthritic symptoms appeared approximately 4 days after monoclonal antibody cocktail infusion. Both mouse hind paws were measured by an electronic calibrator two to three times per week. At termination, the mice were euthanized with CO_2, and blood was collected by heart puncture as described above. The mouse paws were isolated by cutting the whole paws off and fixing them in 10% formalin for 24 hours and then in 70% ethanol before embedding in methyl methacrylate plastic. Goldner's staining and counting of infiltrating cells were performed by Charles River Laboratories International, Inc. (Frederick, MD, http://www.criver.com).

Collagen-Induced Arthritis

Fischer rats (Jackson Laboratory; 10 weeks old) were first immunized with mouse collagen II (0.5 mg) injected s.c. After immunization, either untransduced hMSCs, hsTNFR-transduced hMSCs (4×10^6 cells each), or dexamethasone (0.25 μg) was injected i.p. Arthritis was elicited by injecting 0.5 mg of mouse collagen II in 50 μl of sterile phosphate-buffered saline on day 7 directly into the right knee joint cavity. The same volume of phosphate-buffered saline was injected into the left knee as an intraindividual control. Joint swelling was measured at 2-, 4-, and 7-day intervals and reported as a ratio of right knee divided by left knee values.

RESULTS

Mesenchymal Stem Cells Expressing hsTNFR: Characterization, Expression, and Differentiation

Human MSCs were transduced with a replication-defective MuLV vector expressing a fusion protein of hsTNFR linked with the human IgG1 Fc domain with an internal ribosome-binding site initiating the translation of eGFP from a single RNA transcript (Fig. 1A). We compared transduction efficiency after static and centrifugation methods [28]. Transduction efficiency was determined by FACS analysis of eGFP-positive cell populations and mean fluorescence intensity (MFI). Table 1 shows that when centrifugation was used during MuLV transduction, more than 90% of hMSCs were eGFP-positive, whereas without centrifugation, 70% cells were eGFP-positive. Centrifugation also increased MFI as shown in Table 1 (donor 154, 1,395 [centrifugation] versus 385 [static]). Secretion of transgene hsTNFR into the cultured medium was assayed as described. Expression correlated with the percentage of eGFP-positive cells and MFI; the percentage of

Table 1. In vitro hsTNFR expression from hsTNFR-transduced human MSCs

MSCs	Donor	Amount (nanograms per 10^6 cells per 24 hours)	Flow cytometry analysis	
			eGFP-positive cells (%)	Mean fluorescence intensity
Human, untransduced	154, P3	0		
Human, hsTNFR	154, P3	108	70 (no centrif.)	385
Human, hsTNFR	154, P5	117		
Human, hsTNFR	154, P3	403	93 (with centrif.)	1,395
Human, hsTNFR	154, P5	352		
Human, untransduced	219, P1	0		
Human, hsTNFR	219, P1	171		
Human, hsTNFR	219, P2	854		
Human, hsTNFR	219, P3	131	94% (with centrif.)	205
Human, hsTNFR	219, P4	60		
Human, hsTNFR	219, P5	165		
Human, hsTNFR	219, P6	171	99 (with centrif.)	805
Rat, untransduced	15, P3	0		
Rat, hsTNFR	15, P3	>50	ND	ND
Rat, hsTNFR	15, P4	23		
Rat, hsTNFR	15, P5	34		
Rat, hsTNFR	15, P6	48		

Abbreviations: centrif., centrifugation; eGFP, enhanced green fluorescent protein; hsTNFR, human soluble tumor necrosis factor receptor II; MSC, mesenchymal stem cell; ND, not determined; P, number of cell passages.

eGFP-positive cells was stable over cell passage (Table 1; see donor 219, P1 and P6). Similar to hMSCs, rat MSCs also express hsTNFR when transduced with the MuLV vector but to a lesser extent. The data suggest that reduced expression from rat MSCs compared with hMSCs is due to the fact that only hMSCs were optimized for transgene expression using amphotropic retroviral vectors.

Integration of the hsTNFR transgene into the hMSC genome was analyzed by Northern blot analysis using equal amounts of total RNA from untransduced and hsTNFR-transduced hMSCs from two donors. Figure 1B shows a 3.9-kb transcript in the hsTNFR-transduced hMSCs. Overexpression of the transgene did not alter hMSC multidifferentiation potential, as shown by their ability to undergo osteogenesis, adipogenesis, and chondrogenesis (Fig. 1C). The cells were treated (as described in Methods and Materials), and their commitment toward these different differentiation pathways was analyzed for calcium deposition for osteogenic differentiation, Nile Red retention for adipogenic differentiation, and s-GAG content per ng of DNA for chondrogenic differentiation. In all cases, hsTNFR-expressing hMSCs maintained their ability to differentiate into the three lineage cell types and was similar to that observed for untransduced hMSCs, suggesting that overexpression of the transgene did not alter the "stemness" function of hMSCs.

In Vitro Functionality of hsTNFR-Transduced hMSCs

To demonstrate the functionality of hsTNFR-transduced hMSCs, two types of biological assays were performed using conditioned culture supernatants and cellular surface expression (Fig. 2). Culture supernatants were tested for bioactivity by monitoring NO production from cytokine-treated BACs. It has been demonstrated that the treatment of chondrocytes with either IL-1α or TNFα induce nitric-oxide synthetase activity, resulting in NO production [40]. BAC monolayers were prepared and stimulated with either human TNFα or IL-1α in the presence of supernatants collected from hsTNFR-transduced hMSCs and untransduced hMSCs; 24 hours later, nitrite levels were measured by Griess analysis. Whereas NO production was detected when untransduced hMSC supernatants were present, NO production from human TNFα-treated cultures, but not from those with human IL-1α treatment, was almost completely inhibited in the presence of conditioned supernatants from four different hsTNFR-transduced hMSC cultures (Fig. 2A). On a cellular level, hsTNFR-transduced hMSCs failed to induce surface ICAM expression when the cells were exposed to human TNFα (Fig. 2B). Previous published results have demonstrated TNFα-dependent upregulation of ICAM-1 on the surface of hMSCs [41]. We used this fact to determine whether exposure to TNFα would result in ICAM-1 expression in hsTNFR-transduced MSCs compared with untransduced hMSCs. Titration of human TNFα from 0 to 200 units/ml showed a concentration-dependent induction of ICAM-1 expression on untransduced hMSCs with little to no increase on hsTNFR-transduced hMSCs. The above results support the conclusion that the hsTNFR molecule expressed from hsTNFR-transduced hMSCs is biologically active and capable of binding and neutralizing human TNFα-dependent activities.

In Vivo Functionality of hsTNFR-Transduced hMSCs

Three types of assays were used to show the expression, functionality, and potential efficacy of hsTNFR-transduced hMSCs in vivo: the effect of matrix biomaterial and delivery route on transgene expression, neutralization of endogenous mouse TNFα from implanted human TNFα-expressing cells, and the inhibition of cytokine storm after LPS challenge. NOD/SCID mice were selected as the model system since the absence of a functional immune system allows the implantation of human cells [42].

Experiments were performed to detect systemic levels of hsTNFR in vivo using various three-dimensional matrix biomaterial scaffolds and routes of administration. Cryopreserved hsTNFR-transduced hMSCs were injected i.m. into the hind limbs or s.c. to the back of the animal and compared with implantation of cells adhered to various matrix biomaterials. We tested four biomaterials: PGA; CultiSpher-G, macroporous cross-linked gelatin microbeads; human fibronectin-coated porous hydroxyapatite/tricalcium phosphate, ceramic cubes (HA/TCP; 65% HA and 35% TCP); and alginate disks. The results summarized in Figure 3A indicate that i.m. injection of cells alone and s.c. implanted cells seeded onto PGA felt pads gave rise to the highest systemic

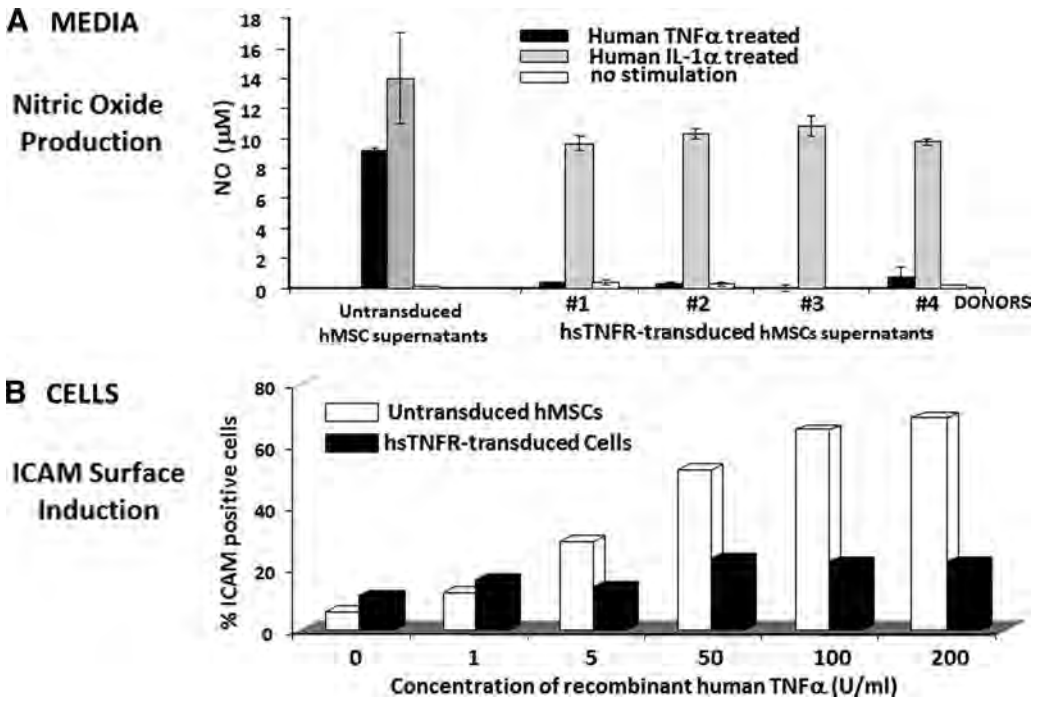

Figure 2. In vitro biological assays show functional hsTNFR activity in hsTNFR-transduced hMSCs. **(A):** hsTNFR-transduced hMSC conditioned medium inhibits hTNFα-mediated nitric oxide release from bovine articular chondrocytes. Griess analysis was done of bovine articular chondrocytes incubated with human TNFα (10 ng/ml) or IL-1α (10 ng/ml) plus conditioned supernatant from hsTNFR-transduced hMSCs (four different donors). Error bars indicate standard deviation ($n = 4$). **(B):** Expression of hsTNFR prevents human TNFα induction of ICAM-1. The indicated amounts of TNFα were added to untransduced or hsTNFR-transduced hMSCs. The cells were harvested 3 days post-treatment, and the percentage of ICAM-1-positive cells was analyzed using fluorescence-activated cell sorting. Analysis was done on a single culture (one well of a six-well panel). Similar results were obtained from hMSC donors 225 and 310. Abbreviations: hMSC, human mesenchymal stem cell; hsTNFR, human soluble tumor necrosis factor receptor II; ICAM, anti-intercellular adhesion molecule; IL, interleukin; NO, nitric oxide; TNFα, tumor necrosis factor-α.

hsTNFR levels (up to 750 pg/ml) within the first week post-treatment (Fig. 3A). Systemic hsTNFR levels declined in the i.m. injected mice in the second week, resulting in systemic levels comparable to CultiSpher (either i.m. or s.c.), s.c. injection of cells alone, implantation of ceramic cubes, or alginate disks. Systemic levels of hsTNFR in mice with PGA felt pad implants plateaued and were sustained for the entire 4-week duration of the experiment. These results suggest that the level of in vivo transgene expression from transduced hMSCs is dependent on the route of delivery and biomaterial used; in this study, cells seeded onto PGA felt pads sustained hsTNFR levels the best. The data suggest that the cells adhere better to PGA felt pads and survive better; in fact, the cells still express hsTNFR in vitro after 4 weeks upon removal from the animals.

As an initial demonstration of efficacy, we tested the ability of hsTNFR expressed from hMSCs to neutralize endogenous human TNFα. To accomplish this, hMSCs expressing human TNFα were injected i.p. followed by s.c. implantation of hsTNFR-transduced hMSCs seeded onto PGA felt pads (Fig. 3B). In these experiments, the animals were split into four groups: implanted with untransduced hMSCs i.p. and s.c. (control); TNFα-transduced hMSCs i.p. and untransduced hMSCs s.c. (TNFα only); TNFα-transduced hMSCs i.p. and hsTNFR-transduced hMSCs s.c. (TNFα/sTNFR); and untransduced hMSCs i.p. and hsTNFR-transduced hMSCs s.c. (sTNFR only). In each of these four groups, sera were collected and pooled to monitor both human TNFα and hsTNFR systemic levels. The levels for both (TNFα and sTNFR) were low in the control group; the TNFα-only and sTNFR-only groups illustrate the systemic level of human TNFα expression possible from the human TNFα-transduced hMSC cell line and the sTNFR expression possible from the hsTNFR-transduced hMSC cell line, respectively. The combination of human TNFα and hsTNFR expression resulted in a 60% reduction in systemic human TNFα and a 50% reduction in systemic hsTNFR. The results suggest the removal and clearance of human TNFα from the systemic circulation caused by the binding to hsTNFR.

An additional demonstration of efficacy was shown through the inhibition of cytokine storm after LPS challenge. LPS acts as the prototypical endotoxin that binds the CD14-TLR4-MD2 receptor complex, promoting the secretion of proinflammatory cytokines. Figure 4A shows the experimental outline. These experiments included a group treated with etanercept (hsTNFR) for comparison with the hMSC-delivered form. It was shown that a sublethal dose of LPS rapidly elevated mouse TNFα levels, peaked in 60–90 minutes and returned to baseline by 24 hours after exposure [43, 44]. TNFα expression induced IL-1α and IL-6 expression. In the experiments summarized in Figure 4, 2 weeks before LPS administration the animals were either s.c. implanted with 4×10^6 hsTNFR-transduced or untransduced hMSCs loaded on PGA felt pads or treated with etanercept twice per week at 4 mg/kg. Mice from untransduced hMSCs (naïve), etanercept, and hsTNFR-transduced hMSCs groups were sacrificed at 0, 1, 6, and 24 hours post-LPS challenge. Mouse sera were harvested and analyzed for the levels of mouse TNFα, mouse IL-1α, mouse IL-6, and hsTNFR as described. Figure 4B shows that the injection of LPS into untransduced hMSC-implanted mice or mice treated

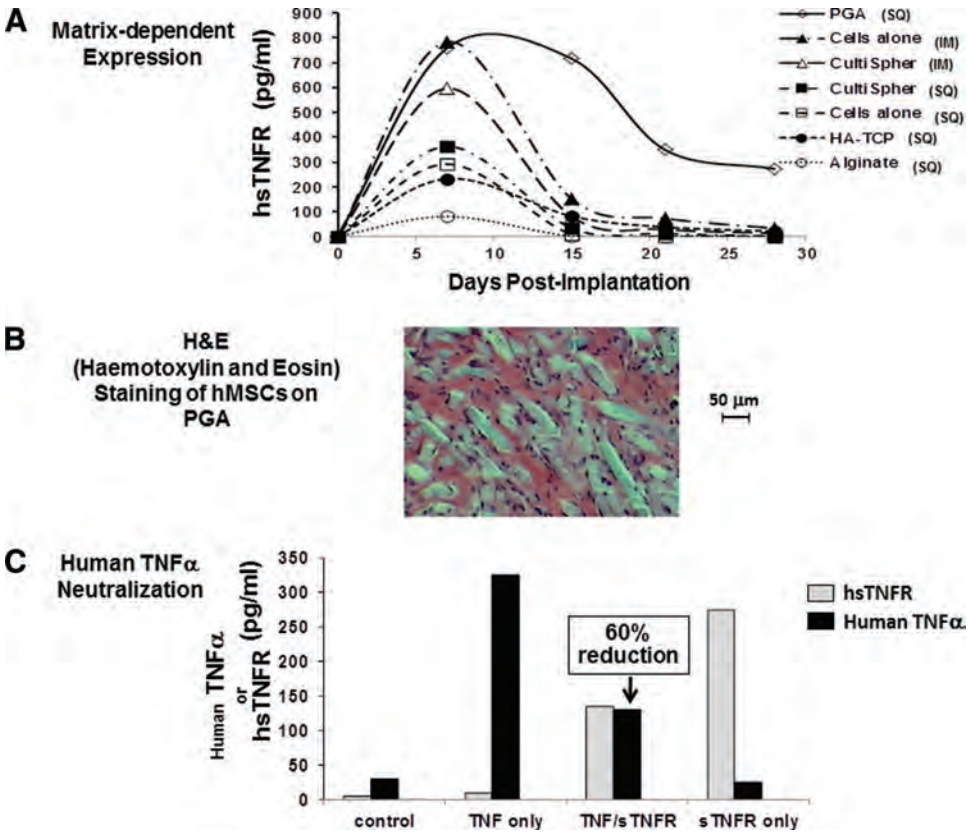

Figure 3. In vivo expression and efficacy of hsTNFR-transduced hMSCs in NOD/SCID mice. **(A):** Systemic hsTNFR level of NOD/SCID mice implanted with hsTNFR-transduced hMSCs. Cryopreserved hsTNFR-transduced hMSCs (donor 154) were carefully thawed and either loaded onto PGA and s.c. implanted (PGA s.c., open diamonds); directly injected into the muscle of the hind limbs (Cells alone (IM), closed triangles); bound to CultiSpher and i.m. implanted (CultiSpher (IM), open triangles); bound to CultiSpher and s.c. implanted (CultiSpher (SQ), closed squares); directly injected s.c. (Cells alone (SQ), open squares); bound to ceramic cubes (HA-TCP, closed circles); or bound to alginate and s.c. implanted (Alginate (SQ), open circles). Blood was collected weekly by retro-orbital puncture. Plasma from each mouse within the same experimental group was pooled and tested for systemic hsTNFR level as described. **(B):** H&E staining of hMSCs on PGA felt pads. **(C):** Ability of hsTNFR-transduced hMSCs to remove systemic human TNFα in NOD/SCID mice. Human TNFα-expressing hMSCs were implanted into NOD/SCID mice followed by the implantation of hsTNFR-transduced hMSCs. Sera were collected from mice on day 3 after hsTNFR-transduced hMSC implantation. Abbreviations: HA, hydroxyapatite; H&E, hematoxylin and eosin; hMSC, human mesenchymal stem cell; hsTNFR, human soluble tumor necrosis factor receptor II; IL, interleukin; IM, intramuscular; PGA, polyglycolide; SQ, subcutaneous; sTNFR, human soluble tumor necrosis factor receptor; TCP, β-tricalcium phosphate; TNFα, tumor necrosis factor-α.

with etanercept caused a rapid increase in mouse TNFα ranging from 3,000 to 5,000 pg/ml in circulation 1 hour post-LPS exposure. The level of mouse TNFα was reduced by 40%–60% in the animals implanted with hsTNFR-transduced hMSCs (reduced to less than 2,000 pg/ml mouse TNFα). At 6 hours post-LPS challenge, mouse TNFα levels from both the untransduced hMSC and transduced hMSC implanted mice decreased to less than 30 pg/ml, but elevated mouse TNFα (7,000–8,000 pg/ml) was seen in the etanercept-treated mice. The levels of mouse IL-1α and mouse IL-6 were not detected at 1 hour (not shown), but at 6 hours post-LPS challenge, significantly less mouse IL-1α and mouse IL-6 were noted in animals implanted with hsTNFR-transduced hMSCs (Fig. 4B, open bars). Etanercept injections reduced mouse IL-1α and mouse IL-6 by 20%, compared with 90% and 50% reduction of mouse IL-1α and mouse IL-6, respectively, by hsTNFR-transduced hMSCs. Measurement of hsTNFR showed a concomitant decrease (450 to 100 pg/ml) in hsTNFR levels in animals receiving hsTNFR-transduced hMSCs, whereas in the etanercept-treated group, similar hsTNFR levels were maintained over the entire 24-hour period (>20,000 pg/ml). No hsTNFR was observed in the naïve group. These data suggest that the reduction in both systemic mouse TNFα and hsTNFR in the animals implanted with hsTNFR-transduced hMSC was due to the binding of these two molecules and clearance of the complex from the circulation; by blocking the in vivo mouse TNFα biological activity, the levels of other proinflammatory cytokines were reduced. In the case of the etanercept treatment, it appears that the mouse TNFα-hsTNFR immunocomplex remains in the circulation. This is in contrast to the complete removal and clearance of TNFα at 6 hours when hsTNFR was expressed from hMSCs. The differential between the amount of mouse TNFα in the naïve and hsTNFR/hMSC groups compared with etanercept-treated group was surprising and suggests that in the etanercept-treated animals, even though TNFα is bound to hsTNFR, the complex is not removed from the circulation and remains longer in the animal's body than TNFα bound to the hsTNFR released from the hMSCs. Whether differential glycosylation or other post-translational modifications are responsible for this difference in clearance is presently not known and requires more analysis. Biocore analysis confirmed the ability of hsTNFR to bind mouse TNFα similar to human TNFα (data not shown).

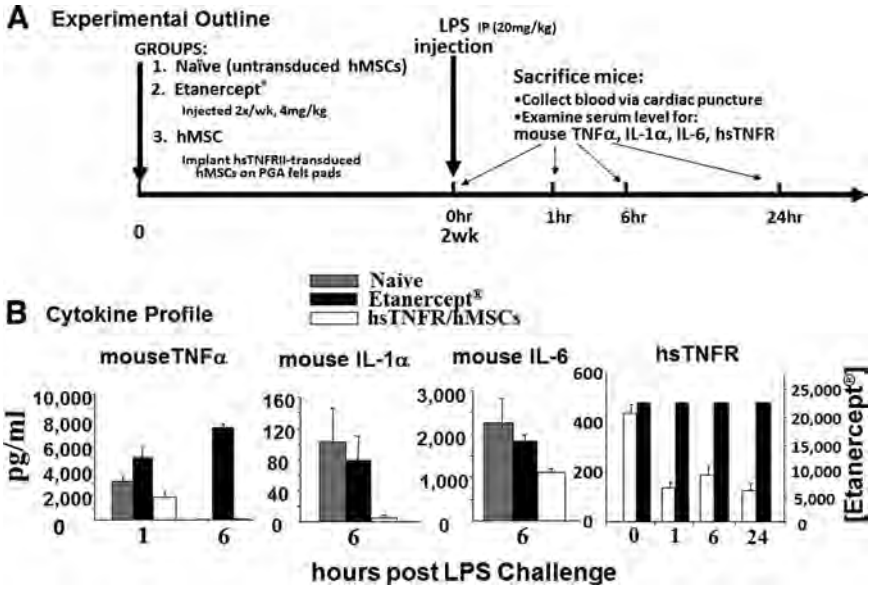

Figure 4. Human sTNFR-transduced hMSCs reduce LPS-induced cytokines in NOD/SCID mice. **(A):** Experimental outline. NOD/SCID mice were s.c. implanted with polyglycolide loaded with untransduced (naïve), hsTNFR-transduced hMSCs or injected s.c. twice per week with 4 mg/kg etanercept as described in Materials and Methods. Two weeks later, mice were i.p. injected with a sublethal dose of LPS (20 mg/kg, 500 μg per mouse). Five to 10 mice were sacrificed from each group prior to or 1, 6, and 24 hours after LPS challenge. Blood was collected by heart puncture. **(B):** Cytokine profile. Plasma was analyzed for circulating proinflammatory cytokines: mouse TNFα, mouse IL-1α, and mouse IL-6, in addition to hsTNFR by enzyme-linked immunosorbent assay as described. Abbreviations: hMSC, human mesenchymal stem cell; hr, hour; hsTNFR, human soluble tumor necrosis factor receptor II; IL, interleukin; IP, intraperitoneal; LPS, lipopolysaccharide; TNFα, tumor necrosis factor-α; wk, week.

hsTNFR-Transduced hMSCs Prevent Arthritis in Animal Models

We tested the efficacy of hsTNFR-transduced hMSCs in an immune-deficient mouse arthritic model in which an anticollagen type II monoclonal antibody cocktail was administered, followed by a LPS challenge. We failed to induce arthritis in NOD/SCID mice because the animals are deficient in complement 5 (L.D. Schultz, personal communication). This is similar to the DBA/1LacJ mouse that carries a similar mutation [45] and is resistant to collagen-induced arthritis. Following the experimental outline shown in Figure 5A, arthritis was successfully induced in BalbC/SCID mice. The thickness of both hind paws was measured, and the ratio of experimental mouse paw thickness to naïve animal paw thickness is plotted against time up to 20 days after disease induction (Fig. 6A). Seven days prior to antibody administration, the animals were injected i.m. in the hind limbs with either transduced or untransduced hMSCs followed by the antibody cocktail injection. LPS was administered 2 days later. The paws of BalbC/SCID mice implanted with untransduced hMSCs showed significantly increased swelling and redness after disease induction (Fig. 5A, solid circles). Histological analysis of the paws on day 20 demonstrated a $+4$ severity of cartilage destruction with 95% macrophage/10% neutrophil inflammatory cell infiltration (Fig. 5A, arthritic control; untransduced hMSCs). Implantation of hsTNFR-transduced hMSCs on day -7 resulted in little to no ($<$10%) swelling comparable to the naïve paws (Fig. 5A, compare no antibody-induced arthritis [AbIA; open circles] to injected hsTNFR/hMSCs [open triangles]). Furthermore, histological assessment showed no or minimal chondrocyte damage and a lack of infiltrating immune cells in the paws from mice implanted with hsTNFR-transduced hMSCs (Fig. 6A, hsTNFR/hMSCs). The histology is comparable to naïve mice (Fig. 6A, no AbIA induction). ELISA analysis of the mouse plasma on day 20 after disease induction revealed 248 pg/ml ($\pm$ 37) of hsTNFR circulating in mice injected with hsTNFR-transduced cells.

To further show in vivo efficacies, we tested hsTNFR-transduced hMSCs in an immune-competent Fischer rat arthritic model where collagen (the antigen) was injected i.p. on day -30 followed by a boost on day 0 directly into the right knee as shown in the protocol outline (Fig. 5B). The rats were prophylactically treated with either untransduced hMSC, hsTNFR-transduced hMSC, etanercept, or dexamethasone (Dex) on day -7. Swelling in the knee was monitored over 7 days by comparing the ratio of the right knee (antigen injected, inflamed) to the left knee (no antigen injected). Rats with untransduced hMSCs showed greater than 60% swelling in the right knee (Fig. 5B, closed squares). A reduction of 12%–20% (1.4–1.3 swelling ratio) in swelling was observed in rats with either hsTNFR-transduced hMSCs (Fig. 5B, open triangles) or etanercept (Fig. 5B, closed circles) after 7 days. Dex, a potent synthetic glucocorticoid known for its anti-inflammatory and immunosuppressant properties, reduced swelling (1.1 swelling ratio) by more than 70% (Fig. 5B, open squares).

Results from these two animal models using both immune-competent (Fischer rats) and immune-deficient (BalbC/SCID mice) animals demonstrate the anti-inflammatory properties and efficacy of hsTNFR-transduced hMSCs in arthritic models. In addition, the current biologic, etanercept, showed a similar anti-inflammatory/efficacy to hsTNFR-transduced hMSCs in the collagen-induced arthritis (CIA) Fischer rat model. Biocore analysis confirmed the ability of hsTNFR to bind rat TNFα similar to human TNFα (data not shown).

Inflammatory Cytokines Inhibit hMSC Chondrogenic Differentiation

In addition to the known effects TNFα has in arthritis, we tested the effect of human cytokine treatment on hMSC chondrocytic

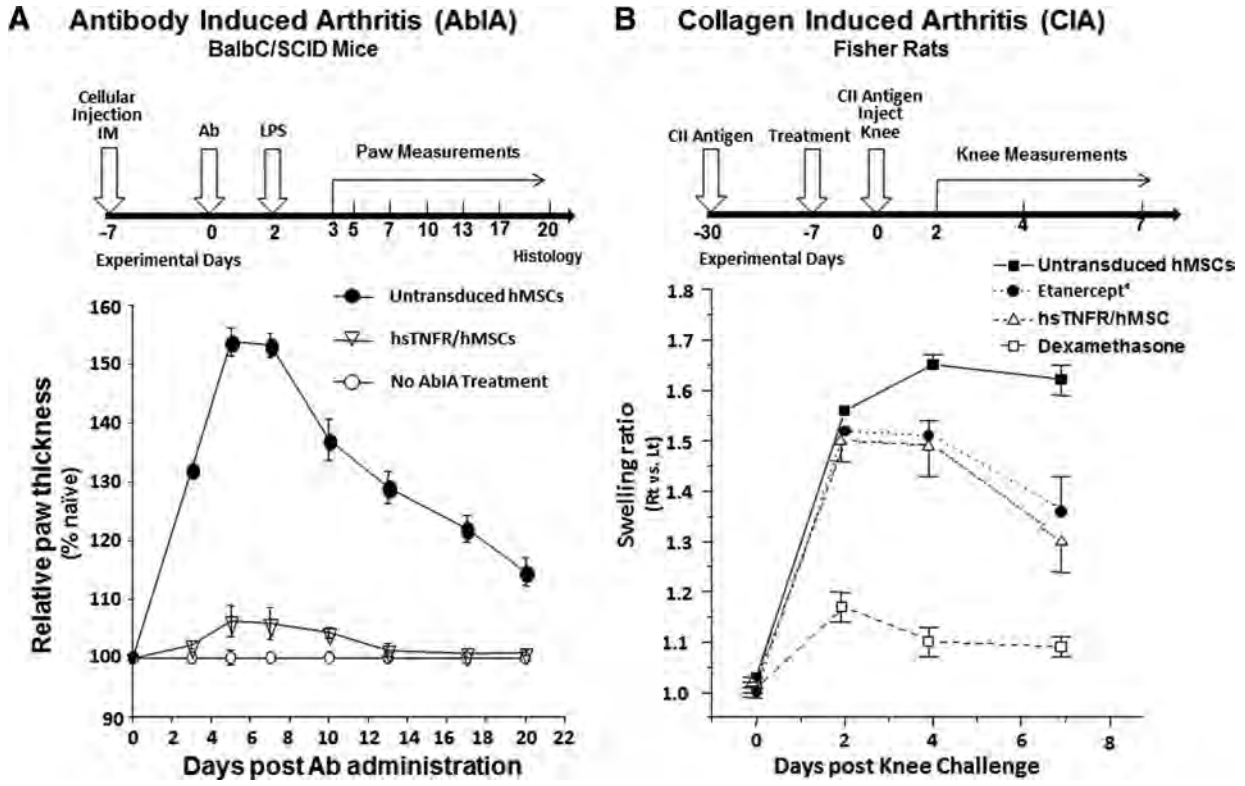

Figure 5. Human sTNFR-transduced hMSCs reduced joint inflammation in immunodeficient and immunocompetent arthritic rodent models. **(A):** AbIA. BalbC/SCID mice were i.m. injected with 4×10^6 untransduced hMSCs or hsTNFR-transduced hMSCs (cellular injection IM in schematic) 7 days before arthritic induction. To initiate arthritis, 300 μl of anticollagen type II monoclonal antibody cocktail (Ab in schematic) was i.v. infused into the mice followed 2 days later by an LPS challenge (50 μg per mouse, i.p.; LPS in schematic). The thickness of hind paws was measured with an electronic calibrator two to three times per week, and the data were plotted as percentages of naïve, untransduced hMSCs ($n = 10$). **(B):** CIA. Fischer rats were immunized s.c. with mouse collagen II (50 mg) 30 days before the initiation of arthritis (CII Antigen in schematic). Seven days before arthritis induction, 4×10^6 untransduced hMSCs or hsTNFR-transduced hMSCs, etanercept (4 mg/kg, injected twice per week), or dexamethasone (0.25 mg) was i.p. injected (Treatment in schematic). Arthritic induction was initiated by the injection of mouse collagen II (0.5 mg in 50 μl of phosphate-buffered saline [PBS]) into the right knee joint cavity (CII Antigen Inject Knee in schematic); for an internal comparison, PBS (50 μl) was injected into the left knee joint cavity. The swelling (measured with an electronic calibrator) of the right knee was compared with that of the left knee, and the ratio was plotted over time for each of the treatments ($n = 10$). Abbreviations: Ab, antibody; AbIA, antibody-induced arthritis; CIA, collagen-induced arthritis; CII, collagen; hMSC, human mesenchymal stem cell; hsTNFR, human soluble tumor necrosis factor receptor II; IM, intramuscular; LPS, lipopolysaccharide; Lt, left; Rt, right.

differentiation. We performed differentiation assays in the presence of three cytokines: two proinflammatory cytokines, TNFα and IL-1α, and one immunostimulatory/immunomodulatory cytokine, IFNγ. The cells were treated with cytokines overnight followed by chondrogenic differentiation (proteoglycans-safranin-O staining) in the absence (no differentiation) and presence (induce differentiation) of tumor growth factor β3 (Fig. 6B). The data clearly show chondrocytic differentiation in untreated and IFNγ-treated hMSCs, but not in TNFα- and IL-1α-treated cells. The data support the conclusion that proinflammatory cytokines prevent hMSC differentiation toward the chondrocytic lineage, indicating that blockade of TNFα and IL-1α is critical for chondrocyte regeneration.

Discussion

The discovery of soluble forms of receptor molecules during the initial cloning of cytokine receptors in the late 1980s was surprising and unexpected [46]. However, today, extracellular coding and receptor shedding are recognized as general regulatory mechanisms in many fields including development, immunology, cell signaling, cell adhesion, and the central nervous system (see [47] for review). The potential of using soluble receptor molecules in therapeutics was rapidly realized in HIV/AIDS with soluble CD4 [48, 49], in tumor angiogenesis with soluble vascular endothelial growth factor receptor [50], and in arthritis with soluble tumor necrosis factor receptor [8, 9]. However, many of these soluble receptors exert their therapeutic function locally but are administered systemically. Thus, it would be desirable to target them to preferred sites, especially areas where damaged tissue exists for tissue engineering and regeneration purposes. A lot of supportive data exist for hMSCs "homing" to damaged tissue, and these cells could be an ideal host for local delivery of therapeutic molecules to damaged tissue [51–53].

As a continuing effort to compare efficacy between biologic drugs and cellular drug delivery, we compared engineered adult hMSCs expressing hsTNFR with the commercially available form, etanercept (Enbrel). The experimental data demonstrate sustained expression of hsTNFR from transduced hMSCs with comparable efficacy to etanercept in blocking cytokine induction after LPS challenge in NOD/SCID mice and the inhibition of joint inflammation in CIA in immune-competent Fischer rats. Whereas both hsTNFR-transduced hMSC and etanercept treatments

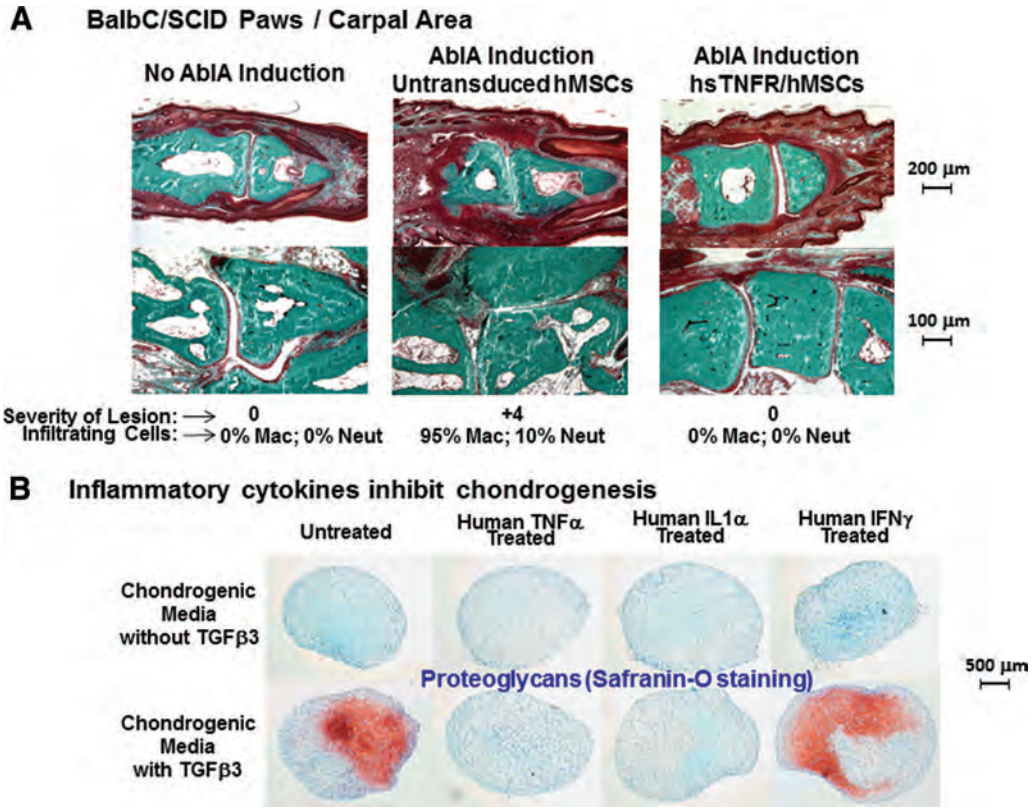

Figure 6. Histology of BalbC/SCID paws and cytokine-dependent inhibition of chondrogenesis. **(A):** BalbC/SCID paws/carpal area. Mouse paws (from Fig. 5A) were removed from animals and fixed with 10% formalin, followed by 70% ethanol before embedding in methyl methacrylate plastic and staining with Goldner's solution. Three panels are shown: phalange joint from untreated animals (no AbIA induction), phalange joint from AbIA-treated animals that were injected i.m. with untransduced hMSCs (AbIA induction, untransduced hMSCs), and phalange joint from AbIA-treated animals that were injected i.m. with hsTNFR-transduced hMSCs (AbIA Induction, hsTNFR/hMSCs). Two magnifications are shown along with visual inspection of the severity of the lesion and percentage count of infiltrating cells. **(B):** Inflammatory cytokines inhibit chondrogenesis. Human MSCs were treated with human proinflammatory (TNFα and IL-1α) cytokines and a immunostimulatory/immunomodulatory (IFNγ) cytokine, followed by assaying for chondrogenic differentiation. Four panels are shown: untreated and cytokine-treated with each panel in the presence (bottom) and absence (top) of the chondrogenic inducer TGFβ3. Safranin-O staining for proteoglycans was performed on all panels as described in Materials and Methods. Abbreviations: AbIA, antibody-induced arthritis; hMSC, human mesenchymal stem cell; hsTNFR, human soluble tumor necrosis factor receptor II; IFNγ, interferon γ; IL, interleukin; Mac, macrophages; Neut, neutrophils; TGFβ3, tumor growth factor β3; TNFα, tumor necrosis factor-α.

showed similar efficacy in the CIA model, differences were observed in LPS challenge experiments in NOD/SCID. After LPS challenge, hsTNFR expressed from hMSCs cleared mouse TNFα faster and thereby reduced the subsequent induction of mouse IL-1α and mouse IL-6. The data suggest that although both molecules bind and sequester TNFα, hsTNFR expressed from hMSCs cleared the complex from the systemic circulation faster than etanercept and at a systemic concentration 100-fold less than that observed with etanercept (Fig. 4). We have shown a similar comparison with erythropoietin (EPO) in that EPO expressed from engineered hMSCs results in faster kinetics for red blood cell generation after administration of a lethal dose of phenylhydrazine compared with recombinant EPO protein [54]. It is conceivable that maintaining therapeutic protein levels by cell transplantation could avoid bolus injections of therapeutic proteins that may be associated with toxicity.

To our knowledge, this is the first report of expressing hsTNFR in hMSCs; our initial results were published in abstract form [55]. Our results demonstrate the importance of "conditioning" the joint by the removal of TNFα preceding joint repair and regeneration. TNFα not only causes inflammation and inhibition of chrondrocytic differentiation but may also reduce the innate immunosuppression ability of MSCs [56]. Thus, the hsTNFR therapeutic molecule could not only prevent the cytokine cascade responsible for cell proliferation and joint degradation but may also preserve the immune privilege ability of MSCs. Our results differ from others [57–59] in that untransduced hMSCs did not have an innate ability to inhibit paw swelling in the mouse arthritic model. Whether this is due to the source and/or species of MSCs used is presently not known. However, our data agree with others [60, 61] in that MSCs themselves cannot inhibit/attenuate arthritis in animal models. Only when hMSCs were either transduced with hsTNFR (as shown here in Fig. 5) or with IL-10 [60] is attenuation of paw swelling and normal histology observed.

Our observation that TNFα, in addition to causing joint destruction, can also inhibit hMSC differentiation toward the chondrocytic lineage was also observed by others. Initially, observations showed reduced chondrogenesis from osteoarthritic patients, suggesting changes in progenitor cell differentiation [62]. Later reports showed that IL-1α, IL-1β, and TNFα inhibited chondrogenesis in a dose-dependent manner through activation of NF-κB [63], which could be reversed by IL-1Ra and etanercept

in chondrogenic pellet cultures of hMSCs [64]. Our observations on cytokine-specific inhibition of chondrocytic differentiation with proinflammatory (TNFα and IL-1α) but not immune stimulatory cytokines (IFNγ) are in line with these previous observations. This observation further illustrates the dual role TNFα has in joint destruction and regeneration.

Human MSC gene delivery may also improve patient compliance by convenient injection every 3–6 months compared with injection of biologics every other day. In addition, this novel approach replaces individual protein manufacturing that in some cases leads either to inactive proteins or to proteins that require subsequent modifications. Human MSC-based protein delivery has advantages over AAV and adenovirus-mediated in vivo gene delivery, in safety and antidrug responses [65]. Other viral and nonviral methods can be used to introduce foreign genes into hMSCs [66]. The method we have described here, if applied to humans, could use autologous hMSCs, minimizing potential immunogenicity and the possibility of rejection. However, hMSCs are immune-privileged [29, 67–69], supporting the possibility of using allogeneic hMSCs as an off-the-shelf product [70, 71]. Thus, in vivo hMSC-based protein delivery offers several potential advantages over recombinant protein and direct in vivo viral vector delivery of therapeutic proteins. Results from future and ongoing experiments will determine the usefulness of hMSCs as vehicles for therapeutic protein delivery and whether cell-based approaches are competitive with other protein delivery systems such as a newly described particle-based protein delivery system [72–74] that uses inactivated surface modified viral particles and/or virus-like particles as scaffolds to deliver therapeutic biologics.

Conclusion

We demonstrated that a single in vivo implantation of hsTNFR-transduced hMSCs in two different arthritic animal models could reverse/attenuate arthritic inflammation. The attenuation in the rat model showed that cellular delivery of hsTNFR was comparable to the commercially available biologic form. In vitro experiments further substantiated the comparable efficacies between cell-based delivery and the recombinant protein, pointing toward a potential advantage of hMSC delivery in faster TNFα removal from the circulation over the biologic form. If this translates into fewer side effects and/or lower compliance remains to be seen. In either case, these results illustrate the ability of hMSCs to deliver proteins of therapeutic value in vivo and demonstrate their potential clinical utility in osteoarthritis and other TNFα-related diseases where anti-TNFα biologic treatment has shown promise.

Acknowledgments

We thank Curt Civin (Johns Hopkins Oncology Center) for acquisition of human bone marrow aspirates and Diana Buyaner and Richard Terry for technical assistance. This study was conducted as part of the collaborative research program between Novartis Pharma AG and Osiris Therapeutics, Inc.

Author Contributions

L.N.L.: conception and design, collection and/or assembly of data, data analysis and interpretation, manuscript writing; G.W. and K.L.: collection and/or assembly of data, data analysis and interpretation; K.H.: collection and/or assembly of data; E.B.: conception and design, administrative support, data analysis and interpretation; U.J.: conception and design, administrative support, collection and/or assembly of data, data analysis and interpretation; J.D.M.: conception and design, administrative support, collection and/or assembly of data, data analysis and interpretation, manuscript writing.

Disclosure of Potential Conflicts of Interest

E.B. has compensated employment as managing director for TET Systems. U.J. has compensated employment and stock options from Novartis.

References

1 Schaible HG, Segond von Banchet G, Boettger MK et al. The role of proinflammary cytokines in the generation and maintenance of joint pain. Ann NY Acad Sci 2010;1193:60–69.

2 Wajant H, Pfizenmaier K, Scheurich P. Tumor necrosis factor signaling. Cell Death Differ 2003;10:45–65.

3 Black RA, Rauch CT, Kozlosky CJ et al. A metalloproteinase disintegrin that releases tumor-necrosis factor-α from cells. Nature 1997; 385:729–733.

4 Moss ML, Catherine Jin SL, Milla ME et al. Cloning of a disintegrin metalloproteinase that processes precursor tumor-necrosis factor-α. Nature 1997;385:733–737.

5 Sivalingam SP, Thumboo J, Vasoo S et al. In vivo pro- and anti-inflammatory cytokines in normal and patients with rheumatoid arthritis. Ann Acad Med Singapore 2007;36:96–99.

6 Brennan FM, Maini RN, Feldmann M. Role of pro-inflammatory cytokines in rheumatoid arthritis. Springer Semin Immunopathol 1998; 20:133–147.

7 Pedersen SJ, Hetland ML, Sorensen IJ et al. Circulating levels of interleukin-6, vascular endothelial growth factor, YKL-40, matrix metalloproteinase-3, and total aggrecan in spondyloarthritis patients during 3 years of treatment with TNFα inhibitors. Clin Rheumatol 2010;29:1301–1309.

8 Williams RO, Feldmann M, Maini RN. Anti-tumor necrosis factor ameliorates joint disease in murine collagen-induced arthritis. Proc Natl Acad Sci USA 1992;89:9784–9788.

9 Piguet PF, Grau GE, Vesin C et al. Evolution of collagen arthritis in mice is arrested by treatment with anti-tumor necrosis factor (TNF) antibody or a recombinant soluble TNF receptor. Immunology 1992;77:510–514.

10 Keffer J, Probert L, Cazlaris H et al. Transgenic mice expressing human tumor necrosis factor: A predictive genetic model of arthritis. EMBO J 1991;10:4025–4035.

11 Kawane K, Tanaka H, Kitahara Y et al. Cytokine-dependent but acquired immunity-independent arthritis caused by DNA escaped from degradation. Proc Natl Acad Sci USA 2010;107:19432–19437.

12 Moreland LW, Baumgartner SW, Schiff MH et al. Treatment of rheumatoid arthritis with a recombinant human tumor necrosis factor receptor (p75)-Fc fusion protein. N Engl J Med 1997;337:141–147.

13 Gibofsky A, Palmer WR, Keystone EC et al. Rheumatoid arthritis disease-modifying antirheumatic drug intervention and utilization study: Safety and Etanercept® utilization analyses from the RADIUS 1 and RADIUS 2 registries. J Rheumatol 2011;38:21–28.

14 Kull FC Jr., Jacobs S, Cuatrecasas P. Cellular receptor for ^{125}I-labeled tumor necrosis factor: Specific binding, affinity labeling, and relationship to sensitivity. Proc Natl Acad Sci USA 1985;82:5756–5760.

15 Gattorno M, Picco P, Buoncompagni A et al. Serum p55 and p75 tumor necrosis factor receptors as markers of disease activity in juvenile chronic arthritis. Ann Rheum Dis 1996; 55:243–247.

16 Mazza J, Rossi A, Weinberg JM. Innovative uses of tumor necrosis factor alpha inhibitors. Dermatol Clin 2010;28:559–575.

17 Wallis RS. Tumor necrosis factor antagonists: Structure, function, and tuberculosis risks. Lancet Infect Dis 2008;8:601–611.

18 Scallon B, Cai A, Solowski N et al. Binding and functional comparisons of two types of tumor necrosis factor antagonists. J Pharmacol Exp Ther 2002;301:418–426.

19 Pearl-Yafe M, Mizrahi K, Stein J et al. Tumor necrosis factor receptors support murine hematopoietic progenitor function in the early stages of engraftment. Stem Cells 2010;28: 1270–1280.

20 Samira S, Ferrand C, Peled A et al. Tumor necrosis factor promotes human T-cell development in non-obese diabetic/severe combined immunodeficient mice. Stem Cells 2004; 22:1085–1100.

21 Haque A, Stanley AC, Amante FH et al. Therapeutic glucocorticoid-induced TNF receptor-mediated amplification of CD4+ T cell responses enhances antiparasitic immunity. J Immunol 2010;184:2583–2592.

22 Kayamuro H, Abe Y, Yoshioka Y et al. The use of a mutant TNF-alpha as a vaccine adjuvant for the induction of mucosal immune responses. Biomaterials 2009;30:5869–5876.

23 Calzascia T, Pellegrini M, Hall H et al. TNF-alpha is critical for antitumor but not antiviral T cell immunity in mice. J Clin Invest 2007;117: 3833–3845.

24 Pasparakis M, Alexopoulou L, Episkopou V et al. Immune and inflammatory responses in TNF alpha-deficient mice: A critical requirement for TNF alpha in the formation of primary B cell follicles, follicular dendritic cell networks and germinal centers, and in the maturation of the humoral immune response. J Exp Med 1996;184:1397–1411.

25 Cournoyer D, Toffelmire EB, Wells GA et al. Anti-erythropoietin antibody-mediated pure red cell aplasia after treatment with recombinant erythropoietin products: Recommendations for minimization of risk. J Am Soc Nephrol 2004;15:2728–2734.

26 Kelley G. 1987–2002: 15 years: EPO saga to augur regulatory change? BioPharm International 2002;15:44.

27 Gaspar R, Duncan R. Polymeric carriers: Preclinical safety and the regulatory implications for design and development of polymer therapeutics. Adv Drug Deliv Rev 2009;61:1220–1231.

28 Lee K, Majumdar MK, Buyaner D et al. Human mesenchymal stem cells maintain transgene expression during expansion and differentiation. Mol Ther 2001;3:857–866.

29 Klyushnenkova E, Mosca JD, Zernetkina V et al. T cell responses to allogeneic human mesenchymal stem cells: Immunogenicity, tolerance, and suppression. J Biomed Sci 2005;12:47–57.

30 Djouad F, Bouffi C, Ghannam S et al. Mesenchymal stem cells: Innovative therapeutic tools for rheumatic diseases. Nat Rev Rheumatol 2009;5:392–399.

31 Mosca JD, Hendricks JK, Buyaner D et al. Mesenchymal stem cells as vehicles for gene delivery. Clin Orthop Relat Res 2000;379:S71–S90.

32 Pittenger MF, Mackay AM, Beck SC et al. Multilineage potential of adult human mesenchymal stem cells. Science 1999;284:143–147.

33 Majumdar MK, Thiede MA, Mosca JD et al. Phenotypic and functional comparison of cultures of marrow-derived mesenchymal stem cells and stromal cells. J Cell Physiol 1998; 176:57–66.

34 Forestell SP, Dando JS, Chen J et al. Novel retroviral packaging cell lines: Complementary tropisms and improved vector production for efficient gene transfer. Gene Ther 1997;4: 600–610.

35 Haynesworth SE, Goshima J, Goldberg VM, Caplan AI. Characterization of cells with osteogenic potential from human marrow. Bone 1992;13:81–88.

36 Jaiswal RK, Jaiswal N, Bruder SP et al. Adult human mesenchymal stem cell differentiation to the osteogenic or adipogenic lineage is regulated by mitogen-activated protein kinase. J Biol Chem 2000;275:9645–9652.

37 Barry F, Boynton RE, Liu B et al. Chondrogenic differentiation of mesenchymal stem cells from bone marrow: Differentiation-dependent gene expression of matrix components. Exp Cell Res 2001;268:189–200.

38 Spirito S, Goldberg RL. The ability of nitric oxide (NO) inhibitors to reverse an interleukin-1 (IL-1) induced depression of proteoglycan synthesis is age dependent. Inflamm Res 1997; 46:S131–S132.

39 Bruder SP, Kurth AA, Shea M et al. Bone regeneration by implantation of purified, culture-expanded human mesenchymal stem cells. J Orthop Res 1998;16:155–162.

40 Stadler J, Stefanovic-Racic M, Billiar TR et al. Articular chondrocytes synthesize nitric oxide in response to cytokines and lipopolysaccharide. J Immunol 1991;147:3915–3920.

41 Majumdar MK, Keane-Moore M, Buyaner D et al. Characterization and functionality of cell surface molecules on human mesenchymal stem cells. J Biomed Sci 2003;10: 228–241.

42 Shultz LD, Schweitzer PA, Christianson SW et al. Multiple defects in innate and adaptive immunologic function in NOD/LtSz-scid mice. J Immunol 1995;154:180–191.

43 Waage A. Production and clearance of tumor necrosis factor in rats exposed to endotoxin and dexamethasone. Clin Immunol Immunopathol 1987;45:348–355.

44 Sekut L, Menius JA, Brackeen MF et al. Evaluation of the significance of elevated levels of systemic and localized tumor necrosis factor in different animal models of inflammation. J Lab Clin Med 1994;124:813–820.

45 Wang Y, Kristan J, Hao L et al. A role for complement in antibody-mediated inflammation: C5-deficient DBA/1 mice are resistant to collagen-induced arthritis. J Immunol 2000; 164:4340–4347.

46 Mosley B, Beckmann BP, March CJ et al. The murine interleukin-4 receptor: Molecular cloning and characterization of secreted and membrane bound forms. Cell 1989;59:335–348.

47 Levine SJ. Mechanisms of soluble cytokine receptor generation. J Immunol 2004;173: 5343–5348.

48 Hussey RE, Richardson NE, Kowalski M et al. A soluble CD4 protein selectively inhibits HIV replication and syncytium formation. Nature 1988;331:78–81.

49 Traunecker A, Luke W, Karjalainen K. Soluble CD4 molecules neutralize human immunodeficiency virus type I. Nature 1988;331:84–86.

50 Ogawa T, Takayama K, Takakura N et al. Anti-tumor angiogenesis therapy using soluble receptors: Enhanced inhibition of tumor growth when soluble fibroblast growth factor receptor-1 is used with soluble vascular endothelial growth factor receptor. Cancer Gene Ther 2002;9:633–640.

51 Karp JM, Leng Teo GS. Mesenchymal stem cell homing: The devil is in the details. Cell Stem Cell 2009;4:206–216.

52 Myers TJ, Granero-Molto F, Longobardi L et al. Mesenchymal stem cells at the intersection of cell and gene therapy. Expert Opin Biol Ther 2010;10:1663–1679.

53 Hong HS, Kim YH, Son Y. Perspectives on mesenchymal stem cells: Tissue repair, immune modulation, and tumor homing. Arch Pharm Res 2012;35:201–211.

54 Wang G, Liu LN, Lee K et al. Comparison of drug and cell-based delivery: Engineering adult mesenchymal stem cells to deliver human erythropoietin. Gene Ther Mol Biol 2009; 13:321–330.

55 Liu L, Wang G, Lee K et al. Expression of soluble TNFRII from transduced human mesenchymal stem cells: *In vitro* and *in vivo* efficacy. Blood 1999;94:400.

56 Djouad F, Fritz V, Apparailly F et al. Reversal of the immunosuppressive properties of mesenchymal stem cell by tumor necrosis factor alpha in collagen-induced arthritis. Arthritis Rheum 2005;52:1595–1603.

57 Augello A, Tasso R, Negrini SM et al. Cell therapy using allogeneic bone marrow mesenchymal stem cells prevents tissue damage in collagen-induced arthritis. Arthritis Rheum 2007;56:1175–1186.

58 González MA, Gonzalez-Rey E, Rico L et al. Treatment of experimental arthritis by inducing immune tolerance with human adipose-derived mesenchymal stem cells. Arthritis Rheum 2009;60:1006–1019.

59 Mao F, Xu WR, Qian H et al. Immunosuppressive effects of mesenchymal stem cells in collagen-induced mouse arthritis. Inflamm Res 2010;59:219–225.

60 Choi JJ, Yoo SA, Park SJ et al. Mesenchymal stem cells overexpressing interleukin-10 attenuate collagen-induced arthritis in mice. Clin Exp Immunol 2008;153:269–276.

61 Schurgers E, Kelchtermans H, Mitera T et al. Discrepancy between the in vitro and in vivo effects of murine mesenchymal stem cells on T cell proliferation and collagen-induced arthritis. Arthritis Res Ther 2010;12:R31–R42.

62 Murphy JM, Dixon K, Beck S et al. Reduced chondrogenic and adipogenic activity of mesenchymal stem cells from patients with advanced osteoarthritis. Arthritis Rheum 2002; 46:704–713.

63 Wehling N, Palmer GD, Pilapil C et al. Interleukin-1b and tumor necrosis factor a inhibit chondrogenesis by human mesenchymal stem cells through NF-kB-dependent pathways. Arthritis Rheum 2009;60:801–812.

64 Heldens GT, Davidson EN, Vitters EL et al. Catabolic factors and osteoarthritis-conditioned medium inhibit chondrogenesis of human mesenchymal stem cells. Tissue Eng Part A 2012;18:45–54.

65 Johnston J, Tazelaar J, Rivera VM et al. Regulated expression of erythropoietin from an AAV vector safely improves the anemia of beta-thalassemia in a mouse model. Mol Ther 2003;7:493–497.

66 Partridge KA, Oreffo RO. Gene delivery in bone tissue engineering: Progress and prospects using viral and nonviral strategies. Tissue Eng 2004;10:295–307.

67 Aggarwal S, Pittenger MF. Human mesenchymal stem cells modulate allogeneic immune cell responses. Blood 2005;105:1815–1822.

68 Nauta AJ, Fibbe WE. Immunomodulatory properties of mesenchymal stromal cells. Blood 2007;110:3499–3506.

69 Atoui R, Chiu RCJ. Concise review: Immunomodulatory properties of mesenchymal stem cells in cellular transplantation: Update, controversies, and unknowns. Stem Cells Translational Medicine 2012;1:200–205.

70 Ponce S, Orive G, Hernandez RM et al. In vivo evaluation of EPO-secreting cells immobilized in different alginate-PLL microcapsules. J Control Release 2006;116:28–34.

71 Yanay O, Barry SC, Flint LY et al. Long-term erythropoietin gene expression from transduced cells in bioisolator devices. Hum Gene Ther 2003;14:1587–1593.

72 Mosca JD, Chang YN, Williams G. Antigen-presenting particle technology using inactivated surface-engineered viruses: Induction of immune responses against infectious agents. Retrovirology 2007;4:32–50.

73 Kueng HJ, Leb VM, Haiderer D et al. General strategy for decoration of enveloped viruses with functionally active lipid-modified cytokines. J Virol 2007;81:8666–8676.

74 Yang Y, Leggat D, Herbert A et al. A novel method to incorporate bioactive cytokines as adjuvants on the surface of virus particles. J Interferon Cytokine Res 2009;29:9–22.